An Endoscopic Robot with Direct-Drive Actuation and Ultra-Steerable Catheters for Transnasal Surgery

Weibo Gao, *IEEE Student Member*, Nitin Srinivasan, Juncheng Zhou, and Hao Su*, *IEEE Senior Member*

***Abstract*—Transnasal endoscopic neurosurgery demands exceptional precision and dexterity to navigate highly constrained intracranial spaces. Existing robotic systems, particularly those employing concentric tube mechanisms, suffer from inherent stiffness, bulky actuation, and limited dexterity, restricting their clinical adoption. In this paper, we present a compact 9-DOF robotic platform integrating ultra-steerable coaxial catheters and direct-drive actuation. Our custom-made direct-drive motors with integrated drivers and sensors provide high-torque, backlash-free actuation, reducing system footprint and enhancing positional accuracy. Benchtop tests showed that our catheter design, featuring coaxial tubes actuated via a push-pull mechanism, achieved a minimal bending radius as 4.2 mm. Other preliminary benchtop experiments validated the precise translation, rotation, and steering capabilities of the robot.**

***Index Terms*—Neurosurgery robot, Ultra-steerable catheter, Direct-drive motor, Minimally invasive surgery.**

I. Introduction

MINIMALLY invasive neurosurgery, such as the transnasal endoscopic pituitary neurosurgery, provides minimally invasive access to the skull base and intracranial structures, significantly reducing surgical trauma compared to traditional open craniotomy procedures [1], [2], [3]. However, these interventions are intrinsically challenging due to highly confined anatomical spaces, intricate tissue structures, and the need for extreme precision to avoid critical tissues such as optic nerves and cerebral vasculature (Fig. 1). Conventional clinical surgical approaches often employ rigid instruments that severely limit the surgeon's maneuverability, posing significant risks of collateral tissue damage and prolonged postoperative recovery. Robotic systems have emerged as a transformative solution, enabling clinicians to perform interventions remotely, thereby minimizing radiation exposure and enhancing procedural precision [4], [5], [6], [7]. Recent advancements in neurosurgery robotics have introduced robotic systems to address these limitations [8], including continuum-based robotic platforms such as the multi-arm concentric tube robots [8], [9], [10]. While concentric tube designs improve dexterity compared to rigid instruments, they remain constrained by inherent limitations: the stiffness of concentrically nested tubes and challenges with elastic instabilities fundamentally restrict achievable curvature and workspace coverage. Additionally, the bulky and complex actuation units necessary for manipulating multiple tubes hinder the practical deployment of these robots in spatially restricted operating rooms and narrow anatomical corridors.

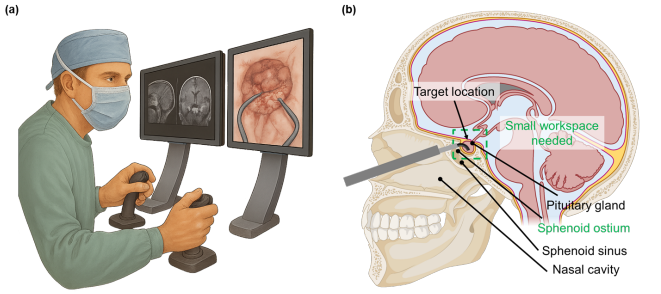

Fig. 1. (a) Robotic endoscopic surgery enables the surgeon to teleoperate the robot while viewing the endoscopic video on a large screen for improved visualization and controlling the motions of surgical tools using joysticks, which eliminates the inaccuracy caused by hand tremors. (b) The endoscopic robot is inserted through a nasal path in the skull. Two steerable catheters enable the surgeon to perform bimanual transnasal skull-base surgeries in a confined corridor without pivoting the instrument against the surrounding brain tissue.

In this study, we present a compact 9-DOF endoscopic robotic system with ultra-steerbale catheters, specifically designed for transnasal neurosurgery, that surpasses the dexterity and workspace constraints of conventional concentric tube robots. Our ultra-steerable catheter employs laser-patterned coaxial tubes actuated by a novel push-pull mechanism driven by customized, compact direct-drive motors. This results in dramatically improved bending capabilities (minimum bending radius $<$5 mm), facilitating precise manipulation within highly constrained intracranial spaces. By minimizing instrument size and maximizing dexterity, our robotic system enables surgeons to achieve enhanced surgical accuracy, reduced invasiveness, and improved patient outcomes, significantly accelerating postoperative recovery. The proposed robotic system thus bridges existing technological gaps, providing a highly maneuverable, compact, and clinically viable solution for minimally invasive transnasal neurosurgery applications, such as pituitary tumor resection and deep-brain electrode implantation.

II. Mechatronics Design of the Endoscopic Neurosurgery Robot

A. Mechanism Design of the 9-DOF neurosurgery Robotic System

Our robotic system integrates an innovative modular design, totaling 9 degrees of freedom (DOFs), specifically optimized for transnasal neurosurgical interventions (Fig. 2). To activate the two ultra-steerable coaxial catheters, where each was controlled independently and provided three degrees of

This work was supported in part by the National Science Foundation (NSF) Cyber-Physical Systems 2344956, National Institutes of Health (NIH) 1R01NS141171-01.

All the authors are with the Lab of Biomechatronics and Intelligent Robotics, Department of Biomedical Engineering, New York University, New York City, NY 11201, USA.

*Corresponding author: hao.su796@ncsu.edu;

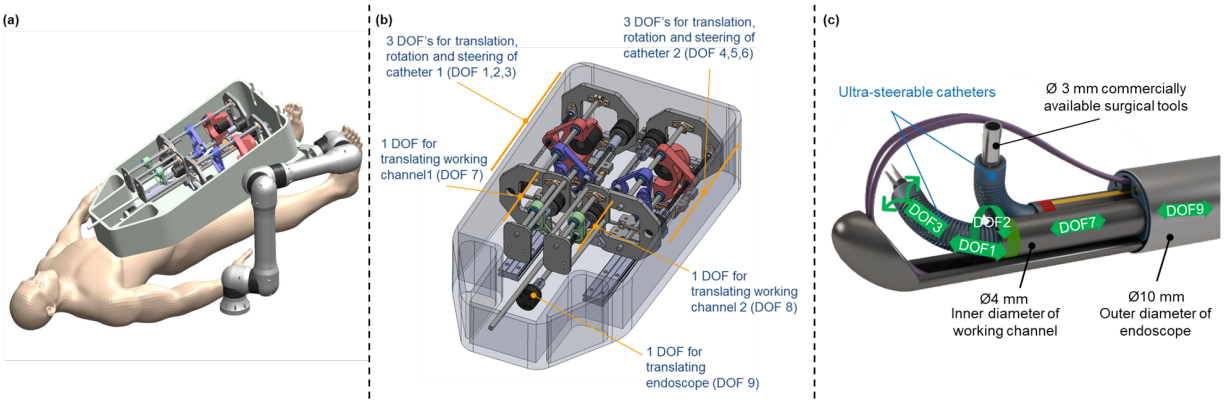

Fig. 2. Mechatronics design of our compact endoscopic neurosurgery robot. (a) Our robot enables teletoperation and is fully portable, which can be mounted on a robot arm or passive arm, facilitating its practicality in the operating room. (b) 9 DOF of the robot for delivering the surgical tools, where DOF 1-3, 4-6 are for insertion, rotation, and steering of two catheters, DOF 7 and 8 are for working channel translation, and DOF 9 is the translation for the endocope. (c) Tip of endoscopic trocar showing robotic arms compatible with ϕ3mm interchangeable tools. The 9 DOFs design enables delivery and dexterous manipulation of commercially available surgical tools in a small corridor. illumination.

freedom—translation, rotation, and steering (i.e., DOF 1-3, 4-6). The steering capability arises from two coaxially aligned tubes, laser-patterned with strategic notches, joined at the distal ends with opposing neutral axes. By applying relative push-pull motions to the tubes, differential bending is achieved with minimal bending radii as small as to 4.2 mm, thus ensuring exceptional dexterity for navigating confined anatomical spaces. To actuate catheter steering and translation, we implemented a motor-driven lead screw mechanism, allowing precise linear displacement. The rotational degree of freedom is facilitated by a compact, hollow-shaft motor coupled with a sliding rod mechanism. This design choice preserves the catheter lumen for surgical tool insertion, maximizing functionality while maintaining a compact overall form factor.

Supporting each catheter is a rigid working channel tube mechanism providing one additional degree of freedom via linear translation for each catheter (DOF 7 and 8). Each reinforcement tube consists of surgical-grade stainless steel and is actuated through a similar lead screw mechanism. These reinforcement tubes enhance catheter stability and structural integrity, enabling precise linear positioning within the transnasal workspace without impeding catheter steerability. Completing the system is an endoscope module (DOF 9), providing the final translational degree of freedom of the cameras. This module integrates both catheters and reinforcement tubes into a rigid yet adjustable linear rail carriage assembly. Movement of this combined module is precisely controlled by another lead screw mechanism. This integrated linear translation allows coordinated depth positioning of the entire surgical instrument assembly relative to the patient's anatomy. The modular nature of this robotic architecture simplifies assembly, calibration, and sterilization. It also enables seamless instrument exchanges during surgical procedures. Collectively, these integrated mechanisms deliver the necessary precision, flexibility, and compactness crucial for enhancing surgical outcomes in transnasal neurosurgery.

B. Electronics Design for the Endoscopic Neurosurgery Robot

The electronics design centers around compact, high-performance direct-drive motors and an integrated custom

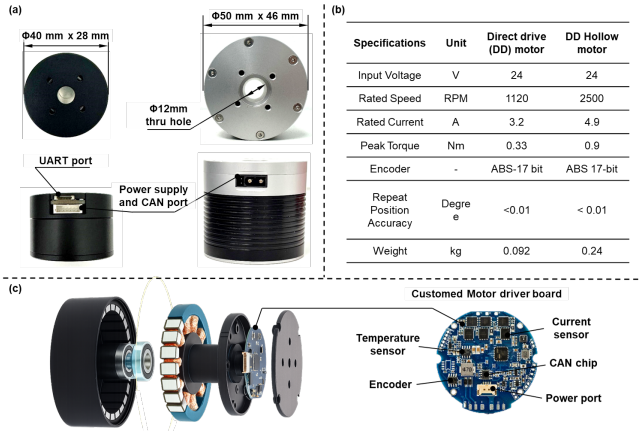

Specifications	Unit	Direct drive (DD) motor	DD Hollow motor
Input Voltage	V	24	24
Rated Speed	RPM	1120	2500
Rated Current	A	3.2	4.9
Peak Torque	Nm	0.33	0.9
Encoder	-	ABS-17 bit	ABS 17-bit
Repeat Position Accuracy	Degre e	<0.01	< 0.01
Weight	kg	0.092	0.24

Fig. 3. (a) dimensions, (b) specs sheet, and (c) exploded view of the two custom-made direct drive actuators.

PCB capable of real-time communication and control. We custom-made two highly integrated, direct-drive BLDC actuators are compact (ϕ40 mm by 28 mm thickness, ϕ50 mm by 46 mm thickness,), featuring built-in motor drivers, dual 16-bit magnetic encoders, current and temperature sensors. The first ϕ40 mm direct-drive motor delivers a peak torque up to 0.33 Nm with a high torque density of 3.67 Nm/kg, and speeds up to 1120 rpm, which was used for all the linear translations and coordination of push-pull movements of the catheter manipulations. We also developed the direct-drive hollow actuators, namely actuators with holes in the center (ϕ12mm) to allow catheters to pass through, thus simplifying and reducing the size of the needed mechanism design of surgical robots. The hollow direct-drive motor delivers a peak torque up to 0.9 Nm with a high torque density of 3.75 Nm/kg, and speeds up to 2500 rpm, which was used rotations of push-pull movements of the catheter. Thanks to the no-gear, direct-drive actuation design, which eliminates the potential mechanical backlash and bulky footprint caused by the gearboxes, our direct drive actuators offer improved accuracy and stability at low rotation speed to address the position accuracy needs. As a result, compared to state-of-the-art low-torque (10 mNm) motors that have to rely on extra gearboxes to deliver sufficient torque, our custom motors deliver high torque (up to 0.33 Nm) for translation and rotation (up to 0.9 Nm) to actuate the ultra-steerable catheter and embedded surgical instruments, while

significantly reducing overall system footprint. Our direct drive actuators are also highly compliant to ensure safe robot-human interaction due to their no-gear design.

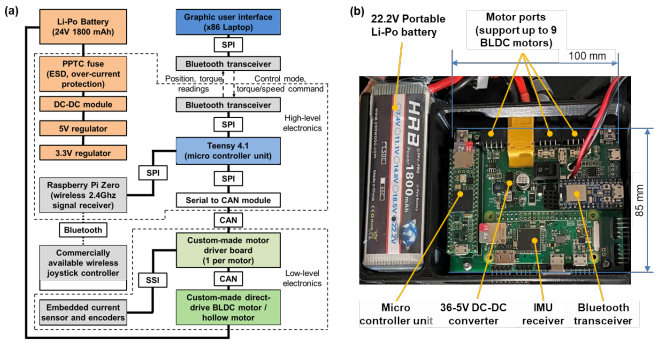

Fig. 4. Our customized PCB enables communication with integrated smart motors via CAN bus protocol.

Our customized two-layer PCB design establishes high-fidelity, high-bandwidth communication between the microcontroller and all nine actuators. Its compact geometry (100 mm length by 85 mm width) greatly assists in reducing the footprint of the robot. The system microcontroller (a Teensy 4.1) regulates the direct drive motors via CAN (Control Area Network) bus protocol. Furthermore, the PCB design can also accommodate different communication protocol electronic units (such as I2C, SPI, UART, USB) and holds a battery port to power all electronic units by reducing the necessity for numerous channels. A 22.2V Li-Po portable battery powers the PCB (including the microcontroller and all the actuators) for nearly five hours, promoting the robot's accessibility and usability for teleoperations.

III. Experiments and Preliminary Results

We conducted preliminary benchtop experiments to validate the functionality and precision of the robotic system, focusing on the actuation accuracy and catheter steerability. An ultra-steerable catheter was actuated via a lead screw-based push-pull mechanism, was initially evaluated to determine the optimal displacement required for maximum catheter bending. Testing revealed that a relative translation of approximately 16 mm between coaxial tubes yielded a minimal bending radius as 4.1 mm, providing excellent dexterity and significantly surpassing the dexterity of conventional rigid tools. (Fig. 5). We also assessed the independent control capabilities of translation, rotation, and steering. Linear motion tests confirmed smooth translation and steering, enabled by precise motor-driven lead screw mechanisms. Rotational control, executed via compact hollow-shaft motors coupled with sliding rod mechanisms, demonstrated consistent 360-degree actuation without interference. These initial results underscore the robotic system's potential to significantly enhance surgical precision and maneuverability in minimally invasive transnasal procedures.

IV. Conclusions and Future Work

This work presents a compact 9-DOF robotic system for transnasal neurosurgery, combining ultra-steerable catheters with custom direct-drive actuations, where the gearless motor

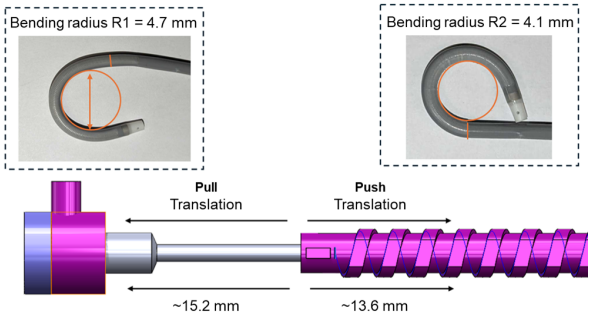

Fig. 5. Push-pull motion and the respective maximum displacement and bending radius of the designed ultra-steerable catheter.

design ensures high torque, low backlash, and a reduced system footprint. Preliminary evaluations confirm accurate motion control and steerability. Future research will involve ex vivo phantoms and in-vivo testing, such as transnasal pituitary tumor resection and deep brain electrode placement. Clinical trials will evaluate improvements in procedural time, targeting accuracy, and surgeon ergonomics. We will also optimize system ergonomics, enhancing haptic feedback mechanisms, and integrating AI-driven algorithms for trajectory planning and navigation [11] for automated robotic assistance.

References

[1] K. Price, J. Peine, M. Mencattelli, Y. Chitalia, D. Pu, T. Looi, S. Stone, J. Drake, and P. E. Dupont, "Using robotics to move a neurosurgeon's hands to the tip of their endoscope," *Science robotics*, vol. 8, no. 82, p. eadg6042, 2023.

[2] H. Su, K.-W. Kwok, K. Cleary, I. Iordachita, M. C. Cavusoglu, J. P. Desai, and G. S. Fischer, "State of the art and future opportunities in mri-guided robot-assisted surgery and interventions," *Proceedings of the IEEE*, vol. 110, no. 7, pp. 968–992, 2022.

[3] H. Su, A. Di Lallo, R. R. Murphy, R. H. Taylor, B. T. Garibaldi, and A. Krieger, "Physical human–robot interaction for clinical care in infectious environments," *Nature Machine Intelligence*, vol. 3, no. 3, pp. 184–186, 2021.

[4] H. Su, M. Zervas, G. A. Cole, C. Furlong, and G. S. Fischer, "Real-time mri-guided needle placement robot with integrated fiber optic force sensing," in *2011 IEEE international conference on robotics and automation*. IEEE, 2011, pp. 1583–1588.

[5] H. Su, D. C. Cardona, W. Shang, A. Camilo, G. A. Cole, D. C. Rucker, R. J. Webster, and G. S. Fischer, "A mri-guided concentric tube continuum robot with piezoelectric actuation: A feasibility study," in *2012 IEEE International Conference on Robotics and Automation*. IEEE, 2012, pp. 1939–1945.

[6] H. Su, G. Li, G. A. Cole, W. Shang, K. Harrington, A. Camilo, J. G. Pilitsis, and G. S. Fischer, "Robotic system for mri-guided stereotactic neurosurgery," *IEEE transactions on biomedical engineering*, vol. 62, no. 4, pp. 1077–1088, 2014.

[7] H. Su, W. Shang, G. Cole, G. Li, K. Harrington, A. Camilo, J. Tokuda, C. M. Tempany, N. Hata, and G. S. Fischer, "Piezoelectrically actuated robotic system for mri-guided prostate percutaneous therapy," *IEEE/ASME transactions on mechatronics*, vol. 20, no. 4, pp. 1920–1932, 2014.

[8] T. L. Bruns, A. A. Remirez, M. A. Emerson, R. A. Lathrop, A. W. Mahoney, H. B. Gilbert, C. L. Liu, P. T. Russell, R. F. Labadie, K. D. Weaver *et al.*, "A modular, multi-arm concentric tube robot system with application to transnasal surgery for orbital tumors," *The International Journal of Robotics Research*, vol. 40, no. 2-3, pp. 521–533, 2021.

[9] J. Burgner, D. C. Rucker, H. B. Gilbert, P. J. Swaney, P. T. Russell, K. D. Weaver, and R. J. Webster, "A telerobotic system for transnasal surgery," *IEEE/ASME transactions on mechatronics*, vol. 19, no. 3, pp. 996–1006, 2013.

[10] H. Su, G. Li, D. C. Rucker, R. J. Webster III, and G. S. Fischer, "A concentric tube continuum robot with piezoelectric actuation for mri-guided closed-loop targeting," *Annals of biomedical engineering*, vol. 44, pp. 2863–2873, 2016.

[11] S. Luo, M. Jiang, S. Zhang, J. Zhu, S. Yu, I. Dominguez Silva, T. Wang, E. Rouse, B. Zhou, H. Yuk *et al.*, "Experiment-free exoskeleton assistance via learning in simulation," *Nature*, vol. 630, no. 8016, pp. 353–359, 2024.